# material chemistry

**DATASET** · SEPTEMBER 2014

READS
15

**3 AUTHORS:**

Somayeh Mohammadi
University of Tehran
**5** PUBLICATIONS **19** CITATIONS
SEE PROFILE

Zahra Kolahdouz
Delft University of Technology
**14** PUBLICATIONS **30** CITATIONS
SEE PROFILE

Shams Mohajerzadeh
University of Tehran
**258** PUBLICATIONS **1,258** CITATIONS
SEE PROFILE

Journal of Materials Chemistry C

RSC Publishing

PAPER

View Article Online
View Journal | View Issue

# Hydrogenation-assisted unzipping of carbon nanotubes to realize graphene nano-sheets

Cite this: J. Mater. Chem. C, 2013, 1, 1309

S. Mohammadi,† Z. Kolahdouz† and S. Mohajerzadeh*

We report the hydrogenation-assisted unzipping of multiwall carbon nanotubes grown on silicon substrates. Carbon nanotubes are formed using hydrogen and acetylene or methane in a direct-current plasma enhanced chemical vapor deposition chamber at a temperature of 650 °C. By patterning the nickel prior to the growth of CNTs, desired patterns are feasible which can be used for unzipping purposes. The unrolling of CNTs is feasible using a mixture of hydrogen and oxygen plasma treatments at temperatures ranging from 200 to 600 °C and in the presence of plasma powers of around 0.3–0.7 watt $cm^{-2}$. By the extended exposure of CNTs to hydrogen plasma at low powers, an anomalous swelling of CNTs has been observed. We believe that the swelling of CNTs is due to the incorporation of H atoms into CNT structure. Scanning electron microscopy, transmission electron microscopy; atomic force microscopy, Raman Spectroscopy and X-ray diffraction analyses have been exploited to investigate the physical properties of the synthesized nano-structures.

Received 13th October 2012
Accepted 7th December 2012

DOI: 10.1039/c2tc00408a

www.rsc.org/MaterialsC



## 1 Introduction

Graphene nano-ribbons (GNRs) are one-dimensional structures with high carrier mobility, ultra high current density, high switching speed, high thermal conductivity and width dependant bandgap characteristics.[1–7] They possess high electron mobility of the order of $1 \times 10^5$ $cm^2$ $V^{-1}$ $s^{-1}$, making them suitable candidates for future nano and bio-electronic devices and circuits. Of especial interest, one can point at the fabrication of field effect transistors and transparent interconnectors. Despite their attractive properties, the formation of such layers seems to be facing severe challenges owing to the complexity of the structure and the fragility of the layers. These restrictions enforce special requirements such high quality, low fabrication costs, ability for large-scale production and also the alignment of GNRs.[5,8] In recent years, new attempts have been developed to obtain GNRs through the unzipping of carbon nanotubes (CNTs) mostly by using a chemical reaction to tear apart CNTs.[9–13] These processes, although successful in the formation of graphene nano-sheets, lead to structures with random order.

In this paper we introduce, for the first time, a direct-current plasma treatment of nanotubes at elevated temperatures to unzip and unroll them and achieve graphene nano-structures. By properly patterning the grown nanotubes and by means of a plasma and mechanical post treatment, it has been possible to arrange the unrolled nanotubes in a near-parallel fashion and with desirable order. While proper use of oxygen and hydrogen treatment would lead to the unzipping of CNTs, a gentle application of hydrogen plasma treatment results in an anomalous swelling of CNTs without being unzipped. In addition, by an intensive hydrogenation treatment it has been possible to split the CNTs into half pieces and observe the inner hollow tubes of these entities. We have also observed a nickel agglomeration at the edges of unzipped nanotubes. Field-emission scanning electron microscopy (SEM), transmission electron microscopy (TEM) and atomic force microscopy (AFM) has been exploited to observe the formation of such nano-structures. Raman spectroscopy and X-ray diffraction (XRD) analyses are employed to investigate the role of hydrogen plasma in the swelling and unzipping of carbon nanotubes.

## 2 Fabrication procedure

In this work, graphene nano-ribbons are formed from the unrolling of carbon nanotubes. For our investigation, carbon nanotubes were grown on p-type single-side polished silicon substrates. Prior to the growth of CNTs, a thin layer of nickel with a thickness of 3–8 nm was deposited on the substrate to act as the catalyst layer. The synthesis of the CNTs was performed at 650 °C using a mixture of $C_2H_2$ (or $CH_4$) and $H_2$ gases in a DC-PECVD reactor. Individual mass flow controllers were used to control the level of the supplied gasses. After a nickel coated sample is placed in the reactor, the surface of the sample is treated with a hydrogen flow at a flow rate of 17 sccm for 15 min, while the substrate temperature is maintained at 650 °C. This step is followed by a 1.5–5 min treatment by hydrogen plasma (plasma current of 25 mA) at the same temperature of the

*Nanoelectronic Center of Excellence, Thin Film and Nano-Electronic Lab, School of Electrical and Computer Engineering, University of Tehran, Tehran, Iran. E-mail: mohajer@ut.ac.ir; Fax: +9821-88011235; Tel: +9821-88011235*

† These authors have the same contribution.

growth in order to create nano islands of Ni. Immediately after the two-step pretreatment, acetylene (or methane) is introduced into the chamber with a flow rate of 5 (12, in the case of methane) sccm for 30 min in order to initiate the growth of CNTs. The flow of hydrogen gas remains constant at 17 sccm. If a highly ordered structure is desired, the nickel layer can be patterned prior to the growth of nanotubes using high precision lithography.

By controlling the growth parameters, such as the thickness of the catalyst layer, hydrogenation time and particularly the type of hydrocarbon gas, the diameter of the CNTs could be controlled. The size, shape and density of the CNTs were determined by SEM. After CNTs are grown in a vertical fashion, they are placed in a reactive ion etching reactor to loosen the silicon at their root side by exposing the sample to $SF_6$ plasma. This is an isotropic etching process, during which the silicon substrate is partially removed while the CNTs remain intact. A mechanical force would be adequate to lay down the CNTs and to place them on a different substrate. Fig. 1 shows how the CNTs are placed horizontally on a silicon sample to become ready for the unzipping process. By proper treatment of nanotubes, it has been possible to unroll and unzip them. Although a gentle exposure to hydrogen plasma leads to an anomalous swelling of CNTs, an intensive exposure results in the complete unzipping of CNTs.

## 3 Results and discussions

The physical structure of CNTs has been extensively investigated using SEM. Microscopy images of Fig. 2 correspond to the formation of vertically aligned nanotubes with different diameters. The top-left image in this figure shows the formation of vertical nanotubes on an interdigital pattern with linear arrays. In addition, the formation of nanotubes with a height of 15 μm and widths of 20 to 100 nm was possible, as seen from various images in this figure. The horizontal placement of CNTs has been feasible using an initial exposure to $SF_6$ plasma to loosen the root side of the CNTs on the silicon substrate. Since the lower part of the CNTs, placed on the silicon substrate was weakened, the CNTs could be easily broken from their root side and fall off on the silicon surface, or on a different substrates, for further processing. To unzip horizontal CNTs, hydrogen plasma is applied at high temperatures. It has been observed that hydrogen plasma at room temperature leads to etching of nanotubes rather than their successful unzipping.

Fig. 3 shows some of the SEM images corresponding to nanotubes with a diameter of 50 nm after being unzipped. The CNTs corresponding to the image in part (a) of Fig. 3 have been merely exposed to hydrogen plasma whereas the CNTs in parts (b) and (c) have been exposed to cyclic hydrogen/oxygen plasma at 300 °C. This cyclic process is based on the quick switching

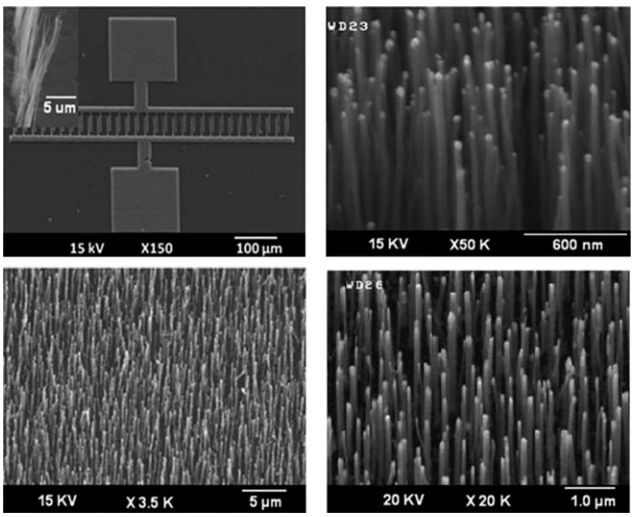


**Fig. 2** SEM images of CNTs with different diameters. The top-left image corresponds to the formation of highly ordered nanotubes on a desired shape and in a linear fashion. Depending on the growth conditions vertical CNTs with heights of 15 μm are feasible, while their diameters could be varied between 20 and 100 nm.

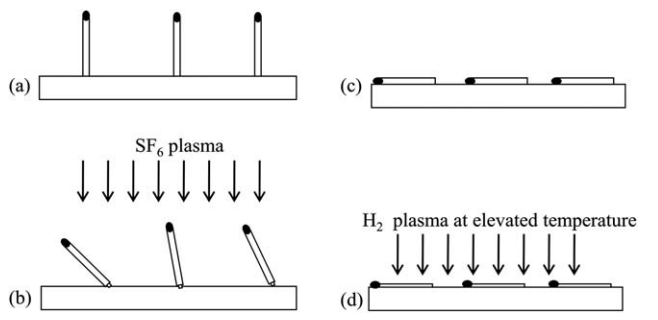


**Fig. 1** The unzipping process of the horizontally placed nanotubes. Once the nanotubes are vertically grown (a), they are laid down by etching the silicon to loosen their roots (b), followed by mechanical rolling (c). The laid nanotubes are then exposed to hydrogen/oxygen plasma in a DC-PECVD reactor and at elevated temperatures to unzip the CNTs (d).

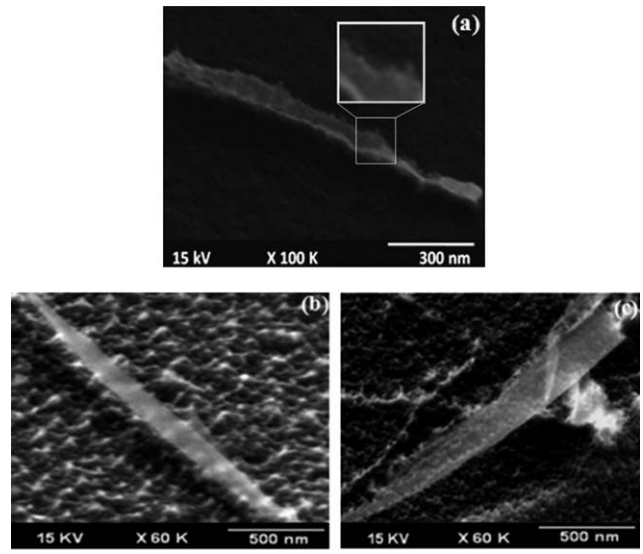


**Fig. 3** A collection of unzipped CNTs at 300 °C, only in hydrogen plasma (a) and in a cyclic hydrogen/oxygen plasma (b and c). The unzipped edges in parts (b) and (c) are much smoother than those in part (a).

 

between hydrogen and oxygen gases during the post-treatment without changing the temperature. The open edges of unzipped CNTs in parts (c) and (d) are smoother than those in part (a). It is important to use a proper mixture of hydrogen and oxygen gases to allow the formation of fully unzipped CNTs with low edge defects. The samples are first exposed to hydrogen plasma followed by another exposure to oxygen plasma under the same thermal conditions. The exact power of the plasma depends on the diameter of the CNTs and we have observed that unzipping of the thicker nanotubes requires higher plasma powers. We believe that oxygen plasma burns the defected parts of the ruptured CNT edges and therefore smoother edges are obtained. In other words, hydrogen is responsible for the unzipping of CNTs, while oxygen removes the highly defective sides to produce smooth edges.

Since hydrogen plays a critical role for the unzipping of nanotubes, its contribution has been studied more thoroughly. For this purpose, we exposed the CNTs to hydrogen plasma at higher temperatures. It is observed that treatment at an elevated temperature leads to more longitudinal unzipping of CNTs with a yield as high as 70%. The SEM images of unzipped CNTs at 500 °C with a plasma power of 0.7 watt $cm^{-2}$ are depicted in Fig. 4. In part (a) of this figure, an SEM image of an individual nanotube has been provided which has been partially unzipped. The CNTs in part (b) and (c) of this figure are split into half pieces during the hydrogenation process and, therefore, the inner hollow tubes of these CNTs are visible. This event is more pronounced in nanotubes with thicker diameters. Parts (d) and (e) of this figure shows collections of unzipped nanotubes on silicon substrates, using the plasma treatment. As seen from these images, all the processed samples show a similar unzipping behavior.

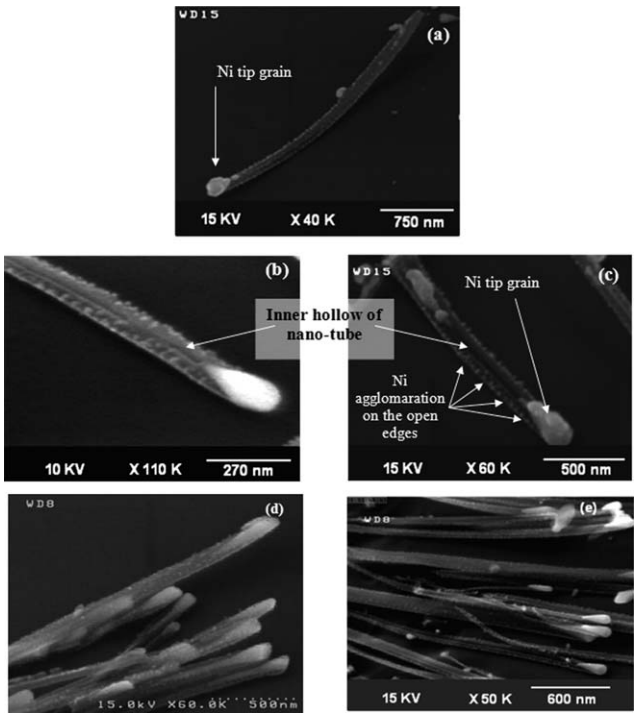


**Fig. 4** SEM images of unzipped CNTs at 500 °C. (a) The formation of a partially unzipped nanotube. (b and c) The central tube of an unzipped structure is quite visible in these images. The presence of white spots at each side of the CNTs is believed to be due to Ni dots. (d) and (e) SEM images of several unzipped CNTs.

Although a high temperature treatment leads to complete longitudinal unzipping or half splitting of CNTs, it causes agglomeration of Ni nano-particles on the edges of unzipped CNTs which have been previously trapped within the CNT structure during the growth process. This phenomenon, which is more expected in low quality CNTs with thicker diameters, has been observed in the samples presented in Fig. 4. The Ni nano-particles, originated from the trapped nickel atoms during the CNT growth, as well as the nickel grain at the tip side of the nanotube, remain as residues in the inner hollow tube of the CNTs and they are easily discernible as bright spots in the SEM images of Fig. 4. The presence of a floating Ni catalyst grain on the top of the unzipped CNTs is a further indication of the unzipping of the CNTs. As stated, the Ni particles were trapped within the CNT structure during the growth process and they are agglomerated during hydrogenation at high temperatures. Ni particles could be intercalated between the walls of CNTs and assist the nanotube longitudinal unzipping. This effect has been previously reported for the intercalation of alkali metals between the coaxial cylinders of CNTs, leading to the unzipping of such nanostructures along their axes.[14]

To better investigate the unzipping process of nanotubes, an AFM apparatus has been exploited. The AFM images of unzipped CNTs are presented in Fig. 5. In accordance with SEM viewgraphs, AFM images verify the inner hollow of the CNTs and the presence of the Ni particles. Part (a) of this figure shows a typical AFM image of an unprocessed nanotube which has been laid down on the silicon substrate. The measurement profile has been inserted in this image for the sake of comparison. In part (b) of Fig. 5, the sample has been exposed to an unzipping treatment and the inner tube of the unzipped CNTs is completely visible in both AFM image and measured profiles, especially when compared to the AFM data of intact CNTs in part (a). More AFM images of thinner diameter CNTs are presented in parts (c) and (d) of this figure. The unzipping of thinner diameter CNTs lead to smoother graphene sheets, which could be partially due to the higher quality of the nanotubes and lesser nickel entrapment in such species. The measured profile of the specimen in these figures shows a height of the order of 4–6 nm, corresponding to the multilayered graphene nano-sheets.

The evolution of graphene layers can be studied more thoroughly by means of a TEM apparatus. For this investigation, we have used a CM30 Philips TEM unit operating at 250 kV. The specimen preparation was possible by a random dispersion of unzipped graphene nano-structures on a copper grid. In Fig. 6 we have collected several TEM images corresponding to various stages of the unzipping of nanotubes. Part (a) in this figure shows the TEM image of half-split nanotubes. The inner hole in the nanotube is discernible in this image. Part (b) in this figure shows the image of partially unzipped CNTs with wrapped edges. In part (c) completely unzipped nanotubes are presented where the graphene nano-ribbons are visible. It should be kept

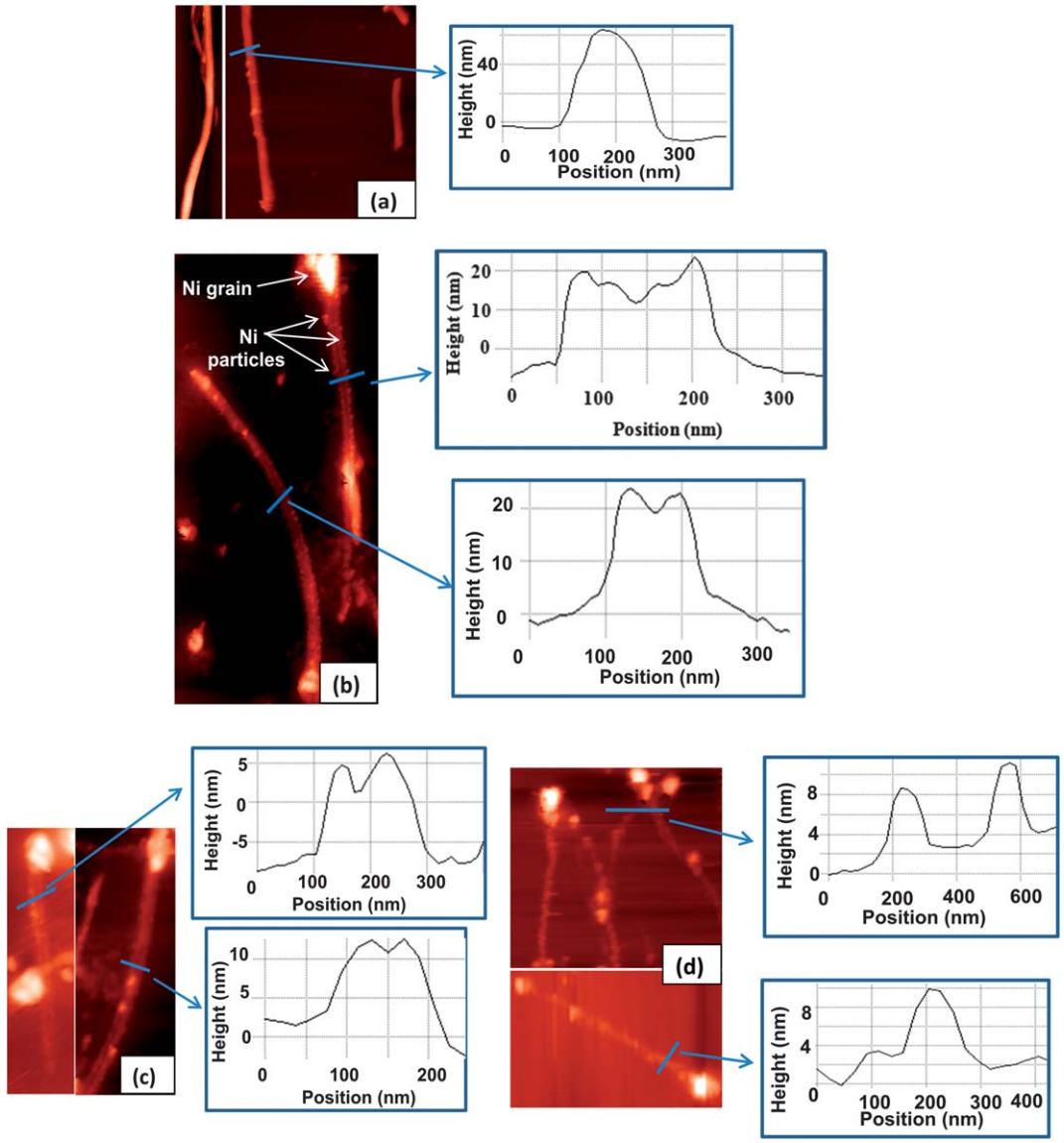


**Fig. 5** A collection of various AFM images. (a) CNTs laid down on the surface of the substrate with diameter of 60 nm. (b) Partially unzipped CNTs with a thick diameter. The inner hollow tube of the original CNT is visible in these images. (c) Unzipped CNTs with a medium diameter. (d) The formation of graphene nanosheets with a height of 4 to 6 nm from unzipped CNTs with a thin diameter.

in mind that during specimen preparation for TEM analysis, the nanoribbons are spread in a random fashion and due to their fragile nature they might fall apart. The presence of white lines between neighboring ribbons depicts the border between such nanostructures. Moreover, the black spots in this figure are due to Ni particles. Although the graphene sheets are bright ribbons in the TEM images, the arrows in part (c) point at certain darker regions which show the places where sheets have been folded. The specimen preparation is responsible for the folding or laying of individual ribbons on one another. As a result, darker regions are observed during TEM analysis.

To better understand the role of hydrogen plasma during the unzipping process, CNTs are exposed to weak hydrogen plasma as opposed to the plasma conditions used in the previous sections. As a result of a lower plasma power of 0.1 W $cm^{-2}$ it has been observed that the carbon nanotubes pass through an anomalous swelling step where the size of nanotubes in their radial direction increases. This swelling is proportional to the duration of the exposure to plasma and longer exposure periods lead to a higher swelling. The SEM images in Fig. 7 show two consecutive steps during the swelling of nanotubes without being unzipped. Part (a) depicts the image for two CNTs crossing one another and prior to any hydrogenation step. Part (b) corresponds to the plasma treatment for 2 min. The sample in part (c) has been exposed to two consecutive steps of hydrogenation for 2 and 3 min (total of 5 min) and the deformation is clearly visible. These treatments have been performed at an elevated temperature of 500 °C to avoid possible damage to the carbon nanotubes. It is worth mentioning that a similar experiment has been conducted by Zhang *et al.* on single-wall

 

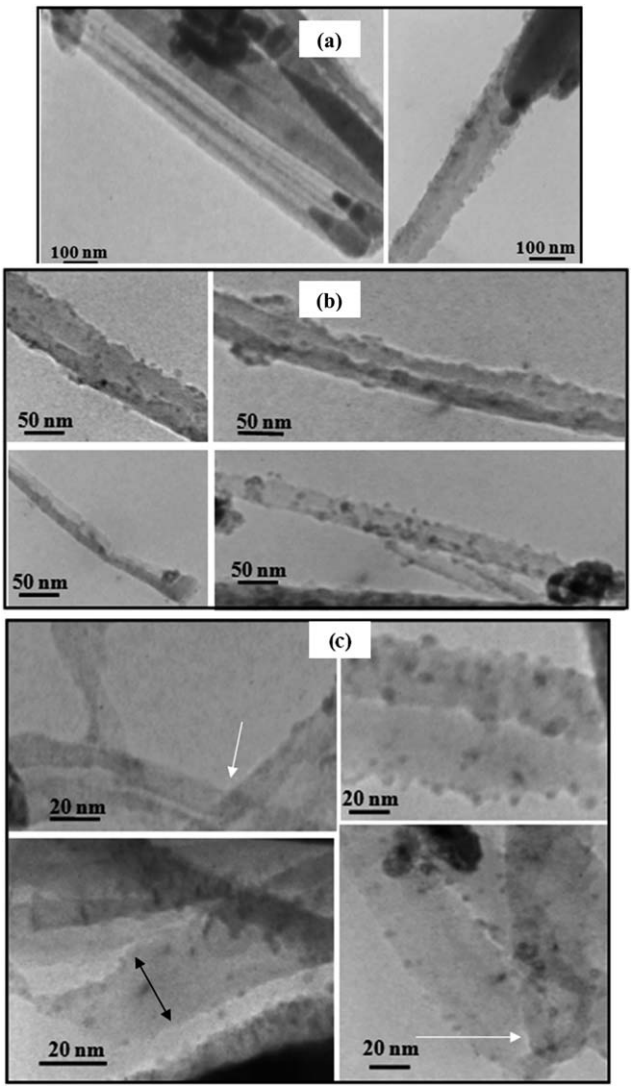


**Fig. 6** TEM images of unzipped CNTs of (a) half-split thick diameter CNTs, (b) unzipped CNTs with wrapped edges, (c) completely unzipped CNTs. Black particles seem to be Ni particles.

nanotubes (SWNT)[15] where the nanotubes have been ruptured. In addition to SEM, we have used further TEM analysis to investigate the swelling of the nanotubes after being exposed to an annealing step. As depicted in Fig. 8, the outer shells of the expanded CNTs become ready for exfoliation, but they are not ruptured. The shaded region on the outer sides of the nanotubes, pointed out by arrows, show the separation of graphite layers from the original nanotubes. It is believed that this swelling is due to chemisorption of hydrogen atoms onto carbon nanotube structure. There have been certain theoretical attempts to distinguish the effect of hydrogen atoms in the CNT structures.[16,17] It is speculated that due to this adsorption, carbon double bonds are broken and hydrocarbonic species ($CH_x$) appear on the surface of CNT walls which, in turn, results in a tensile strain on the carbon bonds. Fig. 7(c) clearly shows how the nanotubes were extended sideways while their length experienced shrinkage. This effect was more visible on the CNTs with shorter lengths as opposed to longer structures.

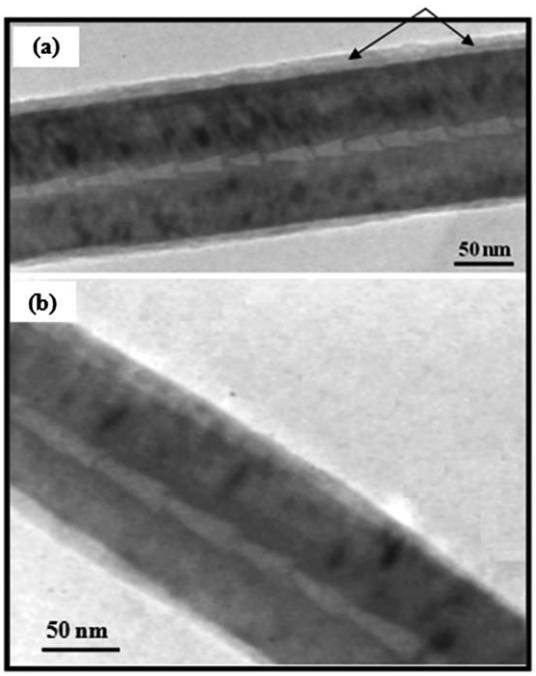


**Fig. 8** TEM images of swollen CNTs during the hydrogenation process. The outer shells are exfoliating. The arrows in part (a), point at the graphite layers which have been separated from the inner parts due to the swelling of CNTs as a result of the annealing process.

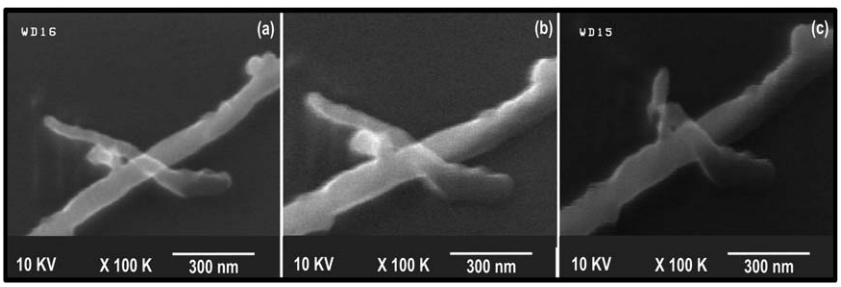


**Fig. 7** Various stages of swelling of CNTs in the hydrogen plasma treatment at an elevated temperature of 500 °C. (a) Prior to hydrogenation, (b) after 2 min hydrogenation, (c) after two consecutive steps of hydrogenation for 2 and 3 min (total of 5 min). This image shows how the crossing CNT was swollen and the main CNT is also thicker.

In addition to electron microscopy images, we exploited Raman Spectroscopy and X-ray diffraction analysis to carry out deeper investigation of such CNT swelling during the hydrogenation process. As depicted in Fig. 9, there is a red-shift in G and D peaks of Raman spectra for the hydrogenated CNTs in comparison with the as-grown ones, which is believed to be due to a tensile strain on the CNT structure, proposing an increase in the length of C–C bonds.[18] The $I_D/I_G$ increment in the hydrogenated CNTs could be assumed to be due to the evolution of defects by H atoms in the CNT structure. More increase in the $I_D/I_G$ ratio for unzipped nanotubes could be an indication of open edges in the graphene sheets.[13] The G′-peak of the as-grown and hydrogenated CNTs is shown in the inset in Fig. 9. One can observe that the G′-peak has slightly broadened and its intensity has increased in hydrogenated CNTs. A gentle red shift is also observable in hydrogenated samples. All these variations in the G′ peak could be due to the tensile stress in the CNT structure,[19] which occurs by the introduction of hydrogen atoms into the structure. We believe that in addition to an increment in the length of carbon bonds due to hydrogenation, the spacing between the $sp^2$ carbon layers increases and the carbon ring possesses a larger radius. This fact is observed from the comparison of the XRD analyses of as-grown and hydrogenated CNTs (Fig. 10). The peak shift from $2\theta = 25.6^\circ$ for as-grown CNTs to $2\theta = 26^\circ$ for hydrogenated CNTs corresponds to an increase in the spacing between carbon layers.[20,21] A negative shift is also observed for the peak at 52°. In fact, there are two peaks around 52° corresponding to the (200) and (004) planes.[20–24] The evolution of the shifts in the XRD spectra is believed to be the expansion of the atomic spacing as a result of plasma treatment. Since the (002) and (004) peaks correspond to similar crystalline directions, the opposite behavior observed for these peaks is not well understood and could be due to the (200) orientation. The arrow in the XRD data, corresponds to the angle related to the (004) and (200) orientations. The opposite behavior of these two peaks could be due to the fact that although the structure is elongated in one direction, in the perpendicular direction it experiences shrinkage. More investigation on this mechanism is underway.

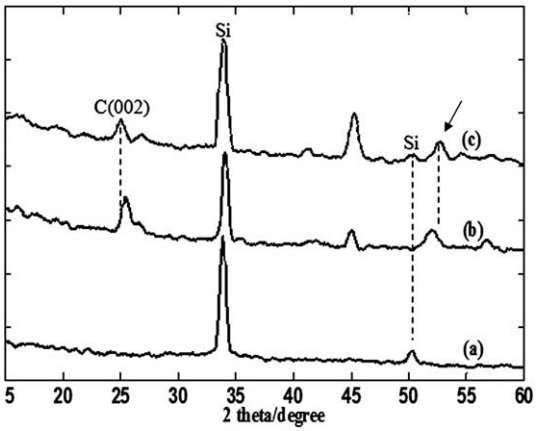


**Fig. 10** The results of XRD analysis on a silicon substrate and the grown nanotubes on such a substrate. (a) The spectrum of silicon substrate prior to any nanotube deposition and processing, serving as a reference. (b) The spectrum of the as-grown CNTs and (c) after being exposed to hydrogen plasma with a power of 0.1 watt $cm^{-2}$ at 500 °C for 3 minutes. A considerable shift is observed for the peak at 26° due to a swelling effect. A negative shift is observed at 53°. These shifts are believed to be due to swelling (shrinkage) in one direction and bond elongation in the other direction. The arrow in this figure points out at an anomalous shift at 52 degrees which could be due to the (200) orientation.

It seems that both hydrocarbon species and the spacing increment between layers could facilitate the unzipping process due to the bond weakening. Under such conditions, intensive hydrogen plasma will initiate longitudinal unzipping of the CNT as depicted in Fig. 11. The arrow in this figure shows the place where the opening of the nanotube has been initiated. Finally, in an attempt to show the ability of this unzipping technique to realize highly ordered arrays of graphene ribbons,

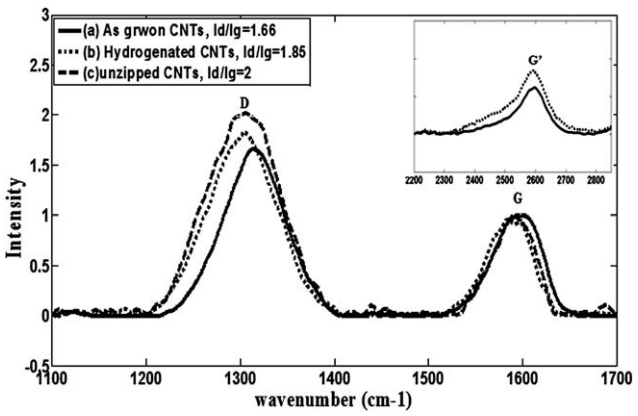


**Fig. 9** Raman spectroscopy results of (a) as grown CNTs, (b) after being exposed to hydrogen plasma with a power of 0.1 watt $cm^{-2}$ at 500 °C for 3 minutes, (c) unzipped CNTs. There is a red-shift in G and D peaks of Raman spectra for the hydrogenated CNTs in comparison with the as-grown ones. The inset in the figure shows the normalized G′-peak of the as-grown and hydrogenated CNTs. The G′ peak slightly broadened and its intensity decreased in the hydrogenated CNTs.

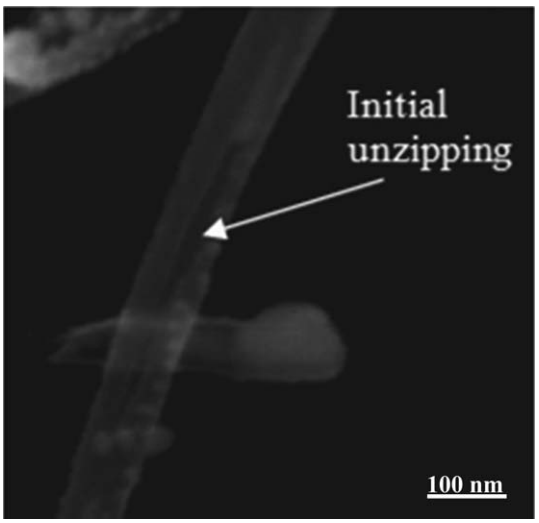


**Fig. 11** Initial unzipping of a swollen CNT using an extensive hydrogenation plasma. The arrow points at the location where the unzipping has been initiated. It seems that nickel dots are agglomerated at the edges of the opened region.

we have grown nanotubes in an isolated and individual fashion to allow proper spacing between neighboring nanotubes once they are laid down. After the separated nanotubes are laid down on the target substrate, they are exposed to the same unzipping process as discussed in previous sections. As can be seen in Fig. 12, by the unzipping of nanotubes with a desired density, it is possible to arrive at a parallel placement of nano-ribbons which are suitable for electronic application. Further investigation on the unzipping mechanism and the nickel leaching from between the layers to the side edges of the unzipped nanoribbons is being pursued.

## 4 Conclusion

In this paper, a novel hydrogenation-assisted post-growth treatment of the nanotubes has been developed to unzip the horizontally placed CNTs. By a mixture of oxygen and hydrogen plasma in a sequential manner, it has been observed that the CNTs have been fully unzipped. The CNTs were halved by hydrogenation at elevated temperature. In addition, an anomalous swelling behavior was observed in the CNTs which have been affected by a mild hydrogenation. This swelling is due to hydrogen accumulation within the CNT wall and is considered to be responsible for a complete longitudinal unzipping of the CNTs. The Raman spectroscopy and TEM analyses of the samples have shown the unzipping process. Apart from unzipping, it has been observed that under less intensive plasma conditions, the hydrogenated nanotubes experience a state of swelling where their length is reduced while their width shows a remarkable increase. This anomalous behavior has been verified by means of scanning electron microscopy and X-ray diffraction technique. Moreover, the unrolling process could lead to the migration of nickel dots from between inner sides of the CNTs towards the opened edges.

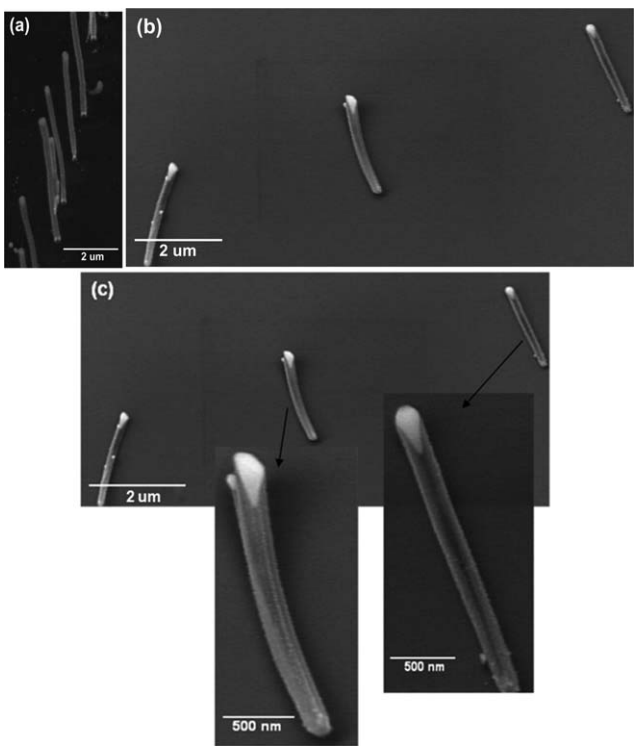


**Fig. 12** SEM images of (a) vertical separately aligned CNTs, (b) horizontal separately aligned CNTs, (c) unzipped separately aligned CNTs. The bottom image shows the presence of hollow tube in the middle of the unzipped nanotube.

## References

1 W. Choi, I. Lahiri and R. Seelaboyina, *Crit. Rev. Solid State Mater. Sci.*, 2010, **35**, 52–71.
2 X. Li, L. Zhang, S. Lee and H. Dai, *Science*, 2008, **319**, 1229–1232.
3 X. Wang, X. Li, H. Wang, J. Guo and H. Dai, *Phys. Rev. Lett.*, 2008, **100**, 206803.
4 Z. H. Chen, Y. M. Lin, M. J. Rooks and P. Avouris, *Phys. E.*, 2007, **40**, 228–232.
5 M. Y. Han, B. Ozyilmaz, Y. Zhang and P. Kim, *Phys. Rev. Lett.*, 2007, **98**, 206805.
6 K. I. Bolotin, K. J. Sikes, Z. Jiang, M. Klima, G. Fudenberg, J. Hone, P. Kim and H. L. Stormer, *Solid State Commun.*, 2008, **146**, 351–355.
7 S. V. Morozov, K. S. Novoselov, M. I. Katsnelson, F. Schedin, D. C. Elias, J. A. Jaszczak and A. K. Geim, *Phys. Rev. Lett.*, 2008, **100**, 016602.
8 L. Jiao, L. Zhang, L. Ding, L. Liu and H. Dai, *Nano Res.*, 2010, **3**, 387–394.
9 Z. Zhang, Z. Sun, J. Yao, D. V. Kosynkin and J. M. Tour, *J. Am. Chem. Soc.*, 2009, **131**, 13460–13463.
10 R. Dhakate, N. Chauhan, S. Sharma and R. B. Mathur, *Carbon*, 2011, **49**, 4170–4178.
11 A. L. Higginbotham, D. V. Kosynkin, A. Sinitskii, Z. Sun and J. M. Tour, *ACS Nano*, 2010, **4**, 2059–2069.
12 L. Jiao, L. Zhang, X. Wang, G. Diankov and H. Dai, *Nature*, 2009, **458**, 877–880.
13 D. V. Kosynkin, A. L. Higginbotham, A. Sinitskii, J. R. Lomeda, A. Dimiev, B. K. Price and J. M. Tour, *Nature*, 2009, **458**, 872–876.
14 G. C. M. Abraham, J. Fernando, J. C.-D. Rodrıguez-Macias, G. Claudia and G. Espinosa, *et al.*, *Nano Lett.*, 2009, **9**, 1527–1533.
15 G. Zhang, P. Qi, X. Wang, Y. Lu, D. Mann, X. Li and H. Dai, *J. Am. Chem. Soc.*, 2006, **128**, 6026–6027.
16 A. h. Park, K. Seo and Y. H. Lee, *J. Phys. Chem. B*, 2005, **109**, 8967–8972.
17 A. Nikitin, H. Ogasawara, D. Mann, R. Denecke, Z. Zhang, H. Dai, K. Cho and A. Nilsson, *Phys. Rev. Lett.*, 2005, **95**, 225507.
18 H. Ko, Y. Pikus and C. Jiang, *Appl. Phys. Lett.*, 2004, **85**, 2598–2600.
19 Q. Li, Y. LanKang, W. Qiu, Y. Li, G. Y. Huang, J. G. Guo1, W. L. Deng and X. H. Zhong, *Nanotechnology*, 2001, **22**, 225704.
20 H. Zhang, G. Lin, Z. Zhou, X. Dong and T. Chen, *Carbon*, 2002, **40**, 2429–2436.
21 X. B. Wu, P. Chen, J. Lin and K. L. Tan, *Int. J. Hydrogen Energy*, 2000, **25**, 261–265.

22 A. Cao, C. Xu, J. Liang, D. Wu and B. K. Wei, *Chem. Phys. Lett.*, 2001, **344**, 13–17.
23 T. I. T. Okpalugo, P. Papakonstantinou, H. Murphy, J. Mclaughlin and N. M. D. Brown, *Carbon*, 2005, **43**, 2951–2959.
24 Y. Maniwa, R. Fujiwara, H. Kira, H. Tou, E. Nishibori, M. Takata, M. Sakata, A. Fujiwara, X. Zhao, S. Iijima and Y. Ando, *Phys. Rev. B: Condens. Matter Mater. Phys.*, 2001, **64**, 073105.